Journal of Hazardous Materials 189 (2011) 158–166

Contents lists available at ScienceDirect

Journal of Hazardous Materials

journal homepage: www.elsevier.com/locate/jhazmat

Stabilization of a magnetic nano-adsorbent by extracted pectin to remove methylene blue from aqueous solution: A comparative studying between two kinds of cross-likened pectin

Roohan Rakhshaee[a,*], Mohammad Panahandeh[b]

[a] Department of Applied Chemistry, Faculty of Science, Islamic Azad University, Rasht Branch, P.O. Box 41335-3516, Rasht, Iran
[b] Environmental Research Institute of Jahad Daneshgahi, Iran

ARTICLE INFO

Article history:
Received 15 December 2010
Received in revised form 25 January 2011
Accepted 6 February 2011
Available online 12 March 2011

Keywords:
Methylene blue uptake
Modified Fe_3O_4 nano-particles
Extracted pectin
Cross-linked

ABSTRACT

The removal of methylene blue (MB) as a cationic dye from aqueous solution by the stabilized Fe_3O_4 nano-particles with the extracted pectin from apple waste (FN-PA) increased due to using the cross-linked forms of the bound pectin on the nano-particles surface by glutaraldehyde (FN-PAG) and adipic acid (FN-PAA) as the cross-linking agents. This increase happened in spite of binding some of the adsorbent functional groups of pectin with nano-particles. It can be due to the local concentrate of other free functional groups after connecting with nano-scale particles. Thermodynamic studies showed that the adsorption equilibrium constant and the maximum adsorption capacities increased with increasing temperature for all of the nano-bioparticles. The kinetic followed the second-order models with the highest rate constants viz. 16.23, 19.76 and 23.04 ($\times 10^{-3}$ g/mg min) by FN-PAA. The adsorption force arrangement of MB by these nano-biosorbents regarding their activation energy was obtained as: FN-PAA > FN-PAG > FN-PA.

1. Introduction

Many industrial productions such as dyestuffs of painting, textiles, paper and pulp, inks, cosmetics, soap, etc., use different synthetic chemical dyes. The common dyes include reactive, disperse, acid, basic and direct dyes which usually have azo groups and aromatic structure which are harmful for human and ecosystem due to their toxicity and stability [1]. The colors in wastewater can also decrease the transparency of water and influence photosynthesis activity which hinders the microbial activities of submerged organisms. The mentioned industry's wastewater must be treated before discharge to minimize the threat to the environment. However, removal of color from wastewater is a great challenge. At present the major techniques for treating dye wastewater are adsorption processes and biological treatment [2–9]. Activated carbon, due to its porous property with large specific surface area, can be an ideal adsorbent for dyes. Natural and synthetic zeolites are also used in water treatment due to their unique structure and cation-exchange properties. Nonetheless, there are disadvantages associated with each of these techniques. For example, activated carbon adsorption only transfers the dyes from the liquid phase to the solid phase [10]. Zeolites have some disadvantages such as poor adsorption capacity and low efficiency [4]. On the other hand, the biological process is difficult to start up and control [10], but the sorption of various dyes onto peat [11] pith [12], wood [13], bagasse fly ash [14] and fungal biomass [15] have been studied. Pectin-rich biomass such as fruit wastes and macro algae can also remove dyes and heavy metals [16,17].

Nanotechnology, as the other new method, is quickly developing in water treatment. At the same time, magnetic nano-adsorbents are composed of magnetic cores and polymeric shells. Compared to the traditional adsorbents, they not only can be manipulated or recovered rapidly by an external magnetic field but also possess quite good performance owing to high efficient specific surface area and the absence of internal diffusion resistance [18–22]. Nano size zero-valent iron has been used to remove acid black dye and the other azo dyes [10,23].

The nano-biosorption methods are especially considered recently. The major advantages of this method are its effectiveness in reducing the concentration of pollutants to very low levels and using inexpensive nano-biosorbent materials [24]. The modified nano-Fe_3O_4 by gum Arabic [24] and polyacrylic acid [25] has

* Corresponding author. Tel.: +98 131 4223152; fax: +98 131 4223621.
E-mail address: rakhshaei@iaurasht.ac.ir (R. Rakhshaee).

0304-3894/$ – see front matter © 2011 Elsevier B.V. All rights reserved.
doi:10.1016/j.jhazmat.2011.02.013

been used to remove pollutants. It was also showed the modification of nanoclays by polysaccharides such as cellulose, chitosan and pectin to uptake pollutants [26].

Pectin is an important polysaccharide constituent of plant cell walls, made of fragments of polygalacturonic acid chains with glycosidic bond α (1 → 4) [27,28]. The degree of pectin methylation (DM) in the cell wall had been expressed as [–$COOCH_3$]/([–$COOCH_3$] + [–COOH]) in the chain [29]. Pectin, due to having functional groups such as carboxyl–carboxylate, can remove dyes and metal ions. In our previous work it was shown that the carboxyl and carboxylate groups of *Lemna minor* s' pectin have the main role to remove cations through an electrostatics attraction [30].

We started the present study with due attention to the separate role and ability of biosorbent's pectin as a biopolymer and nano-magnetic agents as the nano-particles to remove the pollutants such as dyes and metal ions. In other words, although pectin and magnetic nano-adsorbent can uptake dyes, individually, we extracted pectin of apple waste as the main agent of the dye uptake and modified the surface of the synthesized Fe_3O_4 nanoparticles by this pectin and its cross-linked forms to prepare a novel nano-bio-adsorbent and to reach a higher removal efficiency of MB as a cationic dye. These novel nano-bioadsorbents viz. FN-PA, FN-PAG and FN-PAA were characterized by transmission electron microscopy (TEM), X-ray diffraction (XRD) and Fourier transform infrared (FTIR) spectroscopy. Their adsorption capability was studied by the Langmuir equation and kinetic models and the obtained results were compared.

2. Materials and methods

2.1. Synthesis of Fe_3O_4 nanoparticles

The ferric and ferrous ions (molar ratio 2:1) as a mixture of their chloride salts were dissolved in 800 mL deionized water having 0.28 mol Fe^{3+} and 0.14 mol Fe^{2+}. Then 120 mL NH_4OH solution (30%) was added quickly into the iron solution to maintain pH at 10 under vigorous stirring at 25 °C. The co-precipitation of Fe^{2+} and Fe^{3+} was done in the mentioned conditions according to the following equation:

$$2FeCl_3 + FeCl_2 + 8NH_3 + 4H_2O \rightarrow Fe_3O_4 + 8NH_4Cl$$

The precipitates of Fe_3O_4 (confirmed by X-ray diffractometer, Bruker D8-Advance, with Cu Kα radiation, λ = 0.15418 nm) were separated with a magnet and were heated at 80 °C for 30 min, then washed several times with water and ethanol, and finally dried in a vacuum oven at 60 °C [31].

2.2. Preparation of apple sample

The apple waste was collected once, from a factory of fruit juice in November. 50 g of apple sample was washed three times with 2 L deionised water for 30 min and then was air-dried in sun.

2.3. Extraction of pectin from apple waste

30 g of washed apple waste was stirred in 3 L deionized water for 5 h at 80 °C with a mixed solution of $FeCl_3 \cdot 6H_2O$ and $AlCl_3 \cdot 6H_2O$ acidified at pH 3–4 by citric acid to form precipitate [32]. It was then centrifuged at 6000 rpm for 40 min to remove solid particles and was filtered through Whatman filter paper. For pectin precipitation, two volumes of 96% w/w ethanol were added to one volume of pectin extracts, while gently stirring to break up the gelatinous lumps. The obtained mixture was kept for 2 h at 5 °C. Then, pectin gels were centrifuged at 5000 rpm, for 25 min at 20 °C. To remove the mono and disaccharides, the pectin precipitate was washed with 75% ethanol and centrifuged at 4000 rpm for 15 min at 10 °C. Finally, the obtained pectin was dried [33].

2.4. Binding method of pectin to Fe_3O_4 nanoparticles and its cross-linking

For the covalently binding of pectin to the magnetic nanoparticles, we used the method which had been used to connect polyacrylic acid (PAA) on the surface of Fe_3O_4 nanoparticles [25,31]. This selection was done with due attention to the presence of the –COOH groups in pectin similar to PAA where the binding could occur through the reaction between –COOH and the $–NH_2$ groups on the surface of Fe_3O_4 nanoparticles. The amine group could be formed due to the use of concentrated ammonia solution during the co-precipitation of Fe^{2+} and Fe^{3+} ions [31]. On the other hand, the –OH groups are also created on the surface of Fe_3O_4 nanoparticles [24] which can be reacted with –COOH groups of the pectin structure. We also confirmed the successful binding of pectin and its cross-linked forms on the surface of Fe_3O_4 nanoparticles by the FTIR studies of FN-PA, FN-PAG and FN-PAA.

To do the binding processes, 3 g of Fe_3O_4 nanoparticles were mixed with 60 mL of buffer at pH 6 (0.003 M phosphate and 0.1 M NaCl) and 15 mL of carbodiimide solution (0.03 g/mL) as activation agent. After being sonicated for 30 min, 1.5 g of the extracted pectin was added into the mixture. The reaction mixture was sonicated for 50 min at 5 °C. The obtained product is shown as FN-PA.

Cross-linking reactions of pectin were done according to two methods: (a) by adding one third of the obtained FN-PA and 2 mL of 1.2 M (2.4 mmol) glutaraldehyde solution (from Merck) into 120 mL of 2.0 wt% acetic acid solution at 40 °C mixing it for 4 h; the obtained product is shown as FN-PAG (b) by adding one third of the remained FN-PA, 0.35 g (2.4 mmol) of adipic acid (from Merck) and 1 mL of 98% H_2SO_4 into 200 mL of ethanol, with stirring and refluxing at 40 °C for 4 h. The obtained product of this step is shown as FN-PAA. Finally, FN-PA, FN-PAG and FN-PAA which are taken as nano-bioparticles were recovered by a magnet and washed with deionized water.

Fig. 1 shows the cross-linking reactions of pectin by glutaraldehyde (left-hand) and adipic acid (right-hand). As can be seen, the situations of (a) and (a′) shows the possibility and probability of maximum connection between the cross-linking agents and pectin. The reduction of this possibility and probability from the situations (a) and (a′) to (d) and (d′) is seen. The more study about the samples of the cross-linked pectin was performed by FTIR, SHIMADZU-8900.

2.5. Pre-treatment of nano-bioparticles

FN-PA, FN-PAG and FN-PAA were pre-treated by HCl (0.2 M) at pHs 1, 3, 5 and NaOH (0.2 M) at pHs 9, 11 and 12 with range of ±0.1 as six experiments, separately. In order to do these processes, the nano-bioparticle samples (3.0 g) were soaked in HCl and NaOH solutions (0.2 M) at various pHs for 10 h. The samples were then washed three times with distilled water (each time 100 mL for 0.5 min) to remove the excess ions.

2.6. Adsorption experiments

MB ($C_{16}H_{18}ClN_3S$: 319 g/mol) stock solutions were prepared from the analytical grade from Merck in distilled water. A series of 1 L plastic bottles containing 200 mL of MB solution (10–1000 ppm) was prepared. After the pre-treatment process at pH 11.0 ± 0.1 as

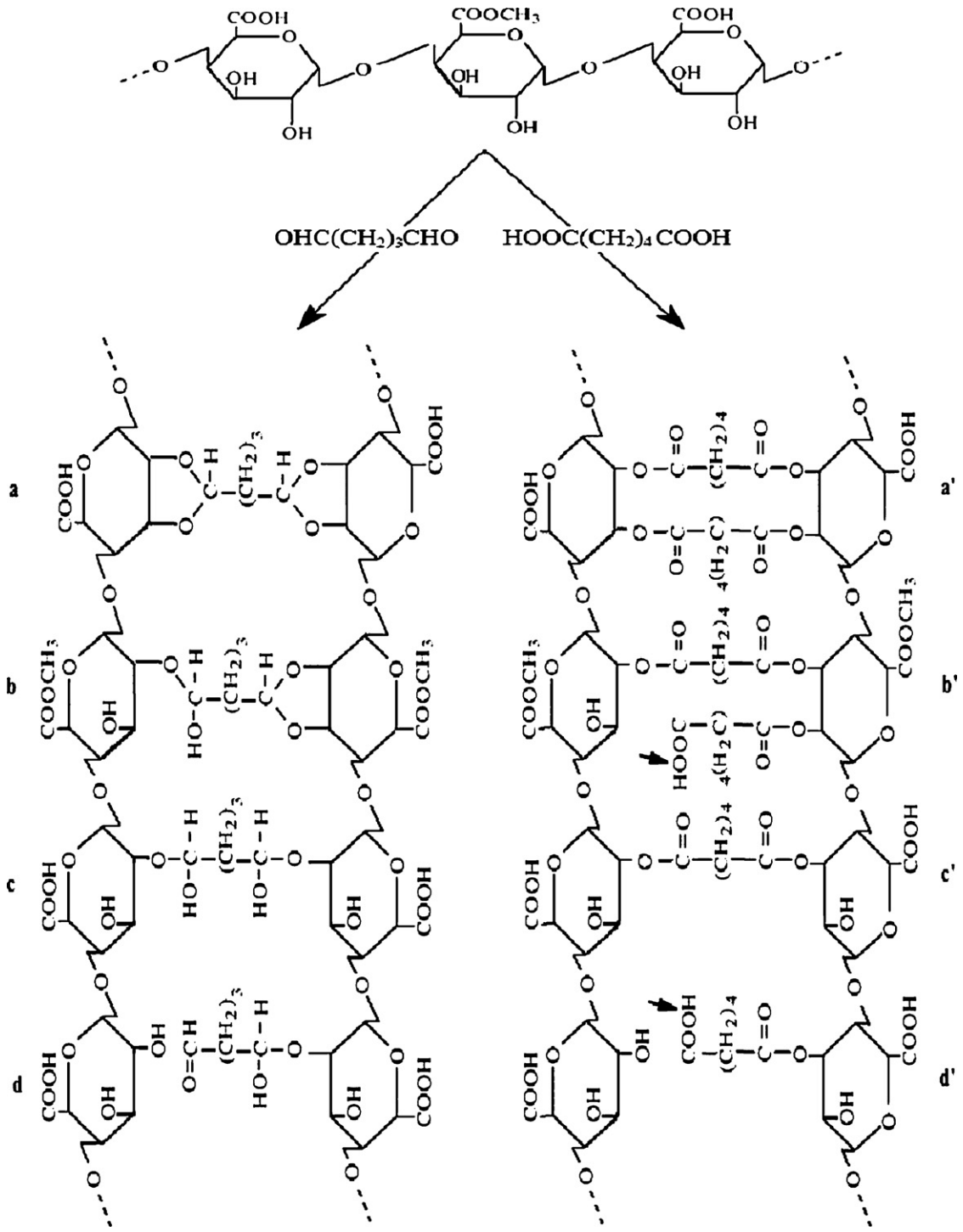

Fig. 1. Cross-linking reactions of pectin by glutaraldehyde (left-hand) and adipic acid (right-hand).

the obtained optimal value (see Fig. 6), the same amounts (5 g/L) of FN-PA, FN-PAG and FN-PAA were separately added into these bottles. The adsorption pH was adjusted 8.0 ± 0.1 as the obtained optimal value (see Fig. 5) for all samples.

The control experiments were performed to eliminate the dye removal effect as the result of the solution acidity, alone, at the different pHs.

The bottles were mixed at 200 rpm and 25 °C. At preselected time intervals, samples were withdrawn and centrifuged with 6500 rpm for 3 min. Then the samples were analyzed for the dye content (C_e) by spectrophotometer (JENWAY, Model 6405) in 660 nm as λ_{max} of MB.

3. Results and discussion

3.1. TEM, XRD and FT-IR studies

Fig. 2 shows the TEM images of the modified Fe_3O_4 nanoparticles with the cross-linked pectin by glutaraldehyde; FN-PAG (A) and adipic acid; FN-PAA (B) as the novel and main nano-biosorbents

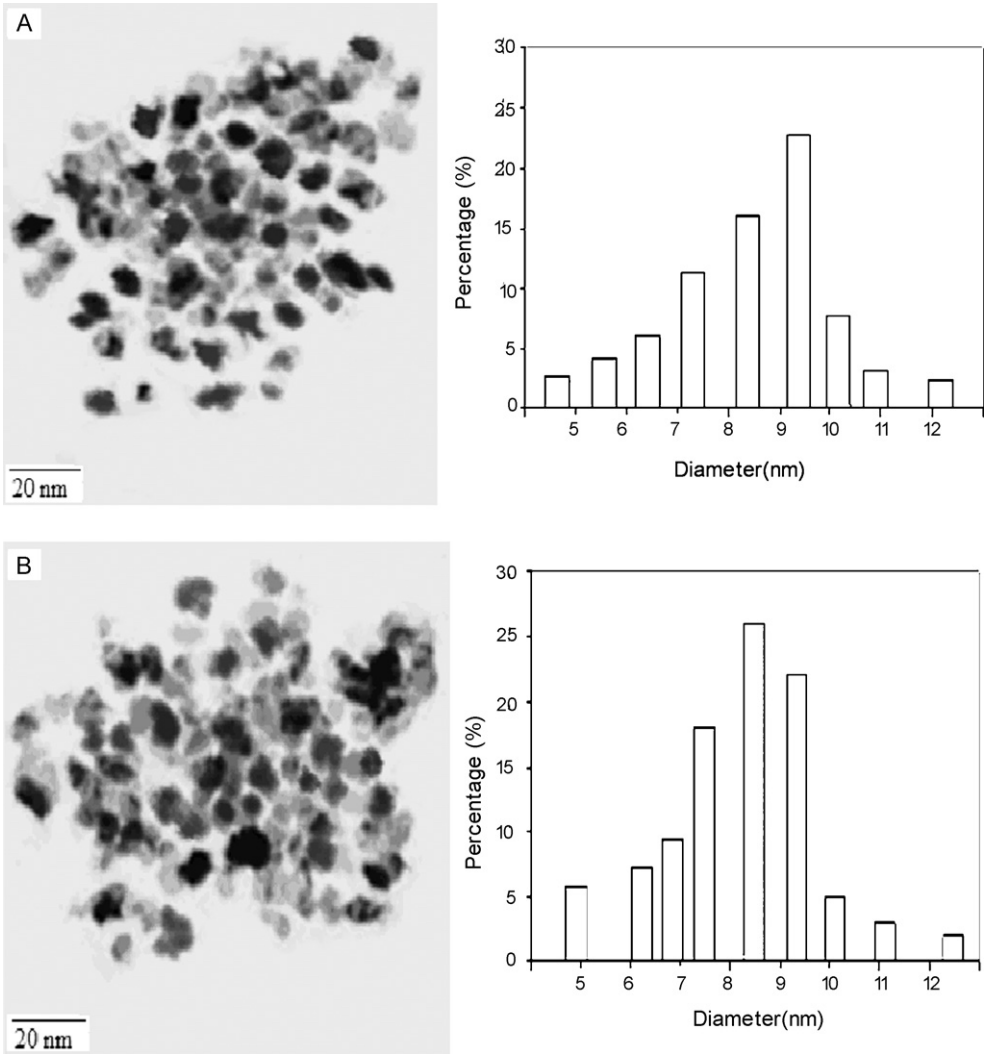

Fig. 2. TEM images of FN-PAG (A) and FN-PAA (B).

in this study. Fig. 3 shows XRD image of Fe_3O_4 nanoparticles (A), pectin-coated Fe_3O_4 nanoparticles without cross-linking; FN-PA (B), FN-PAG (C) and FN-PAA (D). The obtained peaks in the position and the relative intensity did not have obvious differences and all of them were for Fe_3O_4 ($2\theta = 30.1^\circ, 35.5^\circ, 43.1^\circ, 53.4^\circ, 57.0^\circ$, and 62.6°). So these results indicate that the modification of Fe_3O_4 nanoparticles by pectin and cross-linked ones have not changed the crystal structure of nanoparticles, whereas the intensity of the peaks corresponding to the surface functional groups is reduced with using pectin and cross-linking agents. This reduction for FN-PAA is more than that of FN-PAG. The crystal sizes of FN-PAG and FN-PAA were determined from the XRD pattern by using Scherrer's equation; $D = k\lambda/(\beta \cos\theta)$, where D is the average crystalline diameter, k is a constant (0.9 for Cu-kα), λ is the X-ray wavelength (0.15405 nm for Cu-kα), β is the peak width of half-maximum of XRD diffraction lines and θ is the Bragg's diffraction angle in degree. D values were obtained 8.1 and 8.8 nm, respectively, slightly less than that observed from the TEM image.

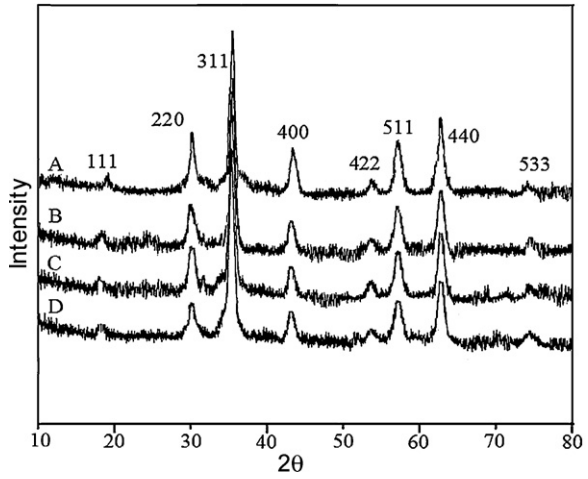

Fig. 3. XRD patterns of Fe_3O_4 nano-particles (A), FN-PA (B), FN-PAG (C) and FN-PAA (D).

Fig. 4 shows the FT-IR spectra of FN-PA (A), FN-PAG (B) and FN-PAA (C). The broad and strong area of absorption between about 3600 and 2500 cm^{-1} in each spectra refers to O–H stretching absorption due to inter and intramolecular hydrogen bonds. This band at 3600–3650 cm^{-1} for FN-PAG is broader and stronger than ones for FN-PA and FN-PAA. It could be due to the presence probability of the created alcoholic –OH groups from the reaction between –CHO groups (from glutaraldehyde) and one –OH group (from pectin) in the situations (b), (c) and (d) in Fig. 1.

On the other hand, the mentioned band for FN-PAA has especially the more breadth at 2430–3350 cm^{-1} which could be due to

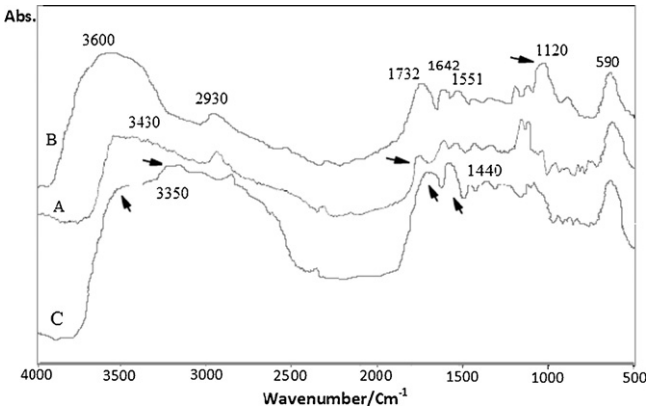

Fig. 4. FT-IR spectra of FN-PA (A), FN-PAG (B) and FN-PAA (C).

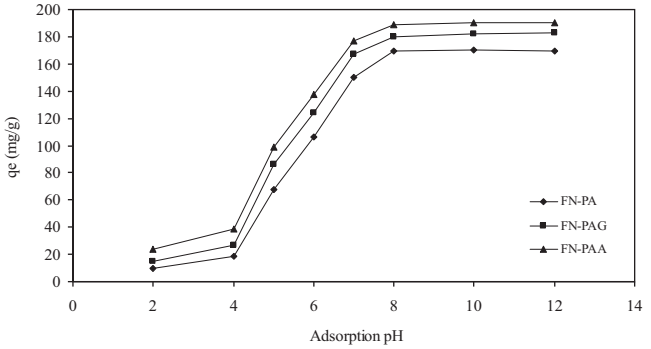

Fig. 5. Effect of initial solution pH (adsorption pH) on the MB uptake by FN-PA, FN-PAG, FN-PAA: pre-treatment pH: 11.0 ± 0.1, initial concentration of MB: 2000 ppm, contact time: 200 min, nano-bioparticles dose: 5 g/L, temperatures: 298 K, agitation rate: 150 rpm.

the presence probability of the –OH groups of the excess –COOH from the non-reacted sites of adipic acid in the situations (b′) and (d′) in Fig. 1 which is added to the alcoholic –OH stretching absorption of the pectin structure. In the case of the esterified sites such as the situations (b) and (b′), an O–CH_3 stretching band would be expected between 2950 and 2750 cm^{-1} due to methyl esters of galacturonic acid. However, due to a large O–H stretching response occurring in a broad region, the O–CH_3 activity is masked and cannot be a reliable indicator of methoxylation. The peaks at 2930 cm^{-1} and 1732 cm^{-1} indicate C–H and C=O (ester carbonyl) absorption, respectively. The stronger peak at nearly 1732 cm^{-1} in the spectra of FN-PAA (C) can be due to the obtained strengthening C=O band (esterified) after the reaction between –COOH groups (from adipic acid) and –OH groups (from pectin) in the situations (a′) to (d′) in Fig. 1.

Furthermore, the absorption of C=O (carboxyl carbonyl) at 1700–1730 cm^{-1} due to the excess –COOH groups in the situations (b′) and (d′) (in addition to –COOH of the pectin structure) is added and composed with the absorption of the carboxyl carbonyl, so they are seen as a stronger band in the spectra of FN-PAA.

The absorption of C=O (aldehyde carbonyl) at near 1725 cm^{-1} due to the presence of the aldehyde group in the situation of (d) for FN-PAG (B) is composed with C=O (carboxyl carbonyl) and C=O (ester carbonyl), so all of them are seen as a peak.

Carboxylate (COO−) groups show two bands, an asymmetrical stretching band at 1642 cm^{-1}, and a weaker symmetric stretching band near 1440 cm^{-1}. These bands for FN-PAA are more intensive because these groups in this nano-bioparticles are more than those of FN-PA and FN-PAG. C=O (ester carbonyl) and COO− are due to the created binding after the reaction between –OH of the nano-particles surface and –COOH of the pectin structure.

The nano-bioparticles have both the dye uptake agents viz. the free –COOH and the amide groups as the binding bridges to the nano-particles viz. the reacted –COOH with –NH_2. The obtained amide group after the reaction between –NH_2 on the Fe_3O_4 nanoparticles and the number of –COOH has two bands at 1632 and 1551 cm^{-1} due to the presence of C=O and N–H, respectively. The band of 1632 cm^{-1} is composed by the band of 1642 cm^{-1} of COO− groups, so they are seen as one band.

Fig. 4 shows the presence of more intensive C=O esterified bands at 1732 cm^{-1} as compared with C=O amide bands at 1632 cm^{-1} for FN-PAG and FN-PAA. On the other hand, the C=O esterified bands for FN-PA (A) viz. the uncross-linked pectin on the nano-particles surface are weaker than those of FN-PAG (B) and FN-PAA (C).

These results can be for the reason that the ratio of the free –COOH (not reacted with –NH_2) to the reacted –COOH viz. the produced amide groups in FN-PA is less than those of the nano-particles with the cross-linked pectin. In other words, the number of the free –COOH in the cross-linked forms can be more than those in the reacted ones.

The weak bands between 1200 and 930 cm^{-1} correspond to the resonance absorption of pyranoid ring. The strong stretching band at 1120 cm^{-1} in spectra of FN-PAG refers to C–O–C which appears after the reaction between –CHO groups (from glutaraldehyde) and two –OH groups (from pectin) in the situations (a) and (b) in Fig. 1. The strong peak at 590 cm^{-1} at spectra in all of the curves could be due to the presence of Fe_3O_4 nanoparticles.

3.2. Effect of adsorption pH

pH of the dye solution for the adsorption process influences not only the surface charge of the nano-biosorbent and the dissociation of functional groups of the active sites on its surface, but also the aqueous chemistry of the dye.

As shown in Fig. 5, the effects of initial solution pH on the MB uptake onto FN-PA, FN-PAG and FN-PAA pre-treated previously at pH 11.0 ± 0.1 as the optimal value (from Fig. 6) were investigated at pH 2–12 as the adsorption pHs.

The electrostatic interaction of cationic MB with the negatively charged groups on the surface of pectin viz. $–O^-$ (from –OH) and $–COO^-$ (from –COOH) can be the main reason of the dye uptake at the different pHs. The sorption of MB on the nanoparticles increased significantly with increasing solution pH from 2.0 to 8.0 and remained approximately constant from 8.0 to 12.0 with a relative maximum. We selected pH of 8.0 ± 0.1 as the optimal value for other experiments. The alkali pHs can be suitable to uptake basic dyes due to the better interactions of the positive groups of

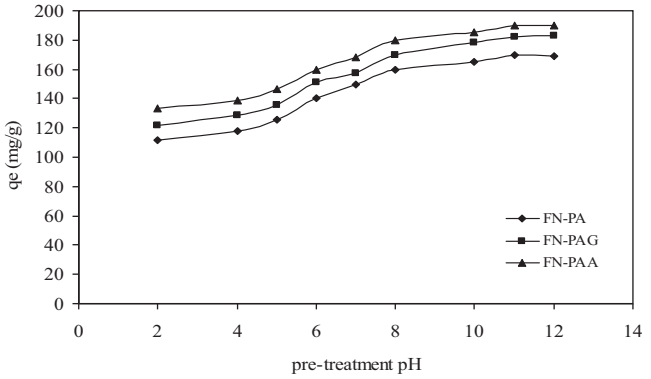

Fig. 6. Effect of pre-treatment pH of FN-PA, FN-PAG and FN-PAA on the MB uptake: adsorption pH: 8.0 ± 0.1, initial concentration of MB: 2000 ppm, contact time: 200 min, nano-bioparticles dose: 5 g/L, temperatures: 298 K, agitation rate: 150 rpm.

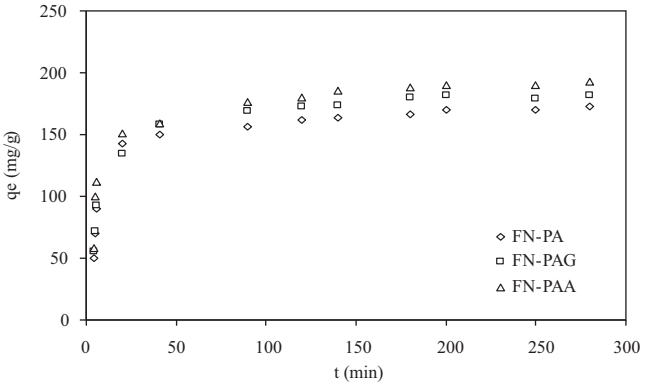

Fig. 7. Effect of contact time on the MB uptake by FN-PA, FN-PAG, FN-PAA. Initial solution pH: 8.0 ± 0.1, pre-treatment pH: 11.0 ± 0.1, initial concentration of MB: 2000 ppm, temperatures: 298 K, nano-bioparticles dose: 5 g/L, agitation rate: 150 rpm.

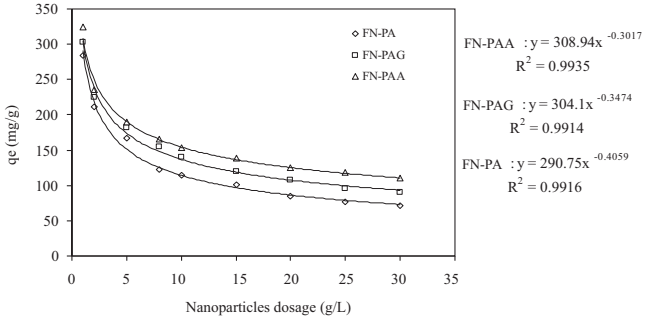

Fig. 8. Effect of nano-bioparticles dose on the MB uptake by FN-PA, FN-PAG, FN-PAA. Initial solution pH: 8.0 ± 0.1, pre-treatment pH: 11.0 ± 0.1, initial concentration of MB: 2000 ppm, contact time: 200 min, temperatures: 298 K, agitation rate: 150 rpm.

dye with the created negative sites in biomass and pectin such as $-COO^-$.

The reason for the low removal at lower pHs could be due to three factors: (1) competition of H^+ with the dye cations of MB (2) repulsive force between $-COOH_2^+$ and $-OH_2^+$ of pectin (not cross-linked and cross-linked form) with the dye cations of MB (3) starting hydrolysis of the pectin structure at the lower pHs [34].

3.3. Effect of pre-treatment pH

As shown in Fig. 6, the pre-treatment pH of FN-PA, FN-PAG and FN-PAA effects remarkably on the MB uptake at pH 8.0 ± 0.1 as the optimal adsorption pH (from Fig. 5). According to Fig. 6, MB uptake increased from 112, 121 and 133 mg/g at the pre-treatment pH of 2.0 to the maximum values viz. 170, 182 and 190 mg/g at the pre-treatment pH of 11.0, by FN-PA, FN-PAG and FN-PAA, respectively.

It could be due to increasing [COO^-] in the pectin structure of FN-PA, FN-PAG and FN-PAA by increasing the pre-treatment pH which reaches the maximum value at pH 11.0 ± 0.1. We also showed in the previous work that [COO^-] in pectin of *Lemna minor* cell wall reaches a maximum at pH 11 to remove the heavy metal ions [30]. So, the nano-bioparticles which were pre-treated at pH 11.0 ± 0.1 had the highest ability to remove MB as a cationic dye.

3.4. Effect of contact time

Fig. 7 shows that the uptake of MB on the nanoparticles increased rapidly within the first 30–50 min and reached an equilibrium after nearly 100 min in the shown conditions. The initial high removal rate of MB within the first 30–50 min was attributed to the high availability of binding sites on the surface of nanoparticles, and the subsequent lower sorption rate decreased the availability of binding sites on the surface of nanoparticles after 50 min due to the removal of the initial MB molecules. The contact time of 200 min was selected in this study to complete the equilibrium, viz the optimum values of MB uptake were obtained after nearly that time. The experimental equilibrium adsorption ($q_{e,exp}$) at 298 K can be determined from Fig. 7 shown in Table 1. $q_{e,exp}$ values at 278 and 313 K (in Table 1) were determined from the similar figures which have not been shown. As can be seen the uptake values of MB in all of the times were obtained as: FN-PAA > FN-PAG > FN-PA.

3.5. Effect of nano-biosorbent dosage

This study was done for the nano-biosorbents with the dosages of 1.0–30.0 g/L at the shown parameters (see Fig. 8). The data were well fitted by the power regression type. As seen in Fig. 8, the sorption capacity of MB on the nano-biosorbent decreased from 284.21 to 125.54 mg/g, 303.11 to 139.01 mg/g and 324.65 to 157.37 mg/g when the dosages of FN-PA, FN-PAG and FN-PAA were increased from 1.0 to 30.0 g/L, respectively. We selected the dosage of 5.0 g/L as an optimum value with the uptake of near to the maximum values, viz. 170, 182 and 190 mg/g for these sorbents, respectively. The decrease of MB uptake with increasing the dosage of nanoparticles is probably due to decreasing the surface area of nano-biosorbents by overlapping or aggregation during the sorption. However, the higher dosage of the sorbent in the solution results in the more availability of the active sites for MB and the higher dye uptake.

3.6. Adsorption studies

Fig. 9a–c shows Langmuir isotherms of MB uptake by FN-PA (a), FN-PAG (b) and FN-PAA (c) with $R^2 > 0.98$. To obtain the Langmuir constants, these isotherms can be transformed to the linearized

Table 1
Adsorption kinetic parameters of MB by FN-PA, FN-PAG and FN-PAA at 278, 298 and 313 K. Initial pH solution: 8.0 ± 0.1, pre-treatment pH: 11.0 ± 0.1, contact time: 200 min, nano-bioparticles dose: 5 g/L, agitation rate: 150 rpm.

Nano-biosorbent	T (K)	First-order kinetic model			Second-order kinetic model			$q_{e,exp}$ (mg/g)
		$k_{1,ads} \times 10^{-3}$ (1/min)	q_e (mg/g)	R^2	$k_{2,ads} \times 10^{-3}$ (g/mg min)	q_e (mg/g)	R^2	
FN-PA	278	8.96	40.38	0.658	8.80	158.98	0.998	157.94
	298	14.18	45.21	0.770	9.51	172.12	0.999	170.12
	313	18.75	54.34	0.689	10.46	191.56	0.997	190.53
FN-PAG	278	15.67	48.69	0.756	12.73	162.98	0.995	161.12
	298	21.22	52.90	0.730	14.69	184.23	0.998	182.11
	313	25.66	65.49	0.659	16.39	194.67	0.996	192.33
FN-PAA	278	22.56	51.89	0.739	16.23	168.47	0.999	166.98
	298	28.65	61.66	0.657	19.76	193.78	0.999	190.55
	313	32.78	78.43	0.678	23.04	206.82	0.996	205.53

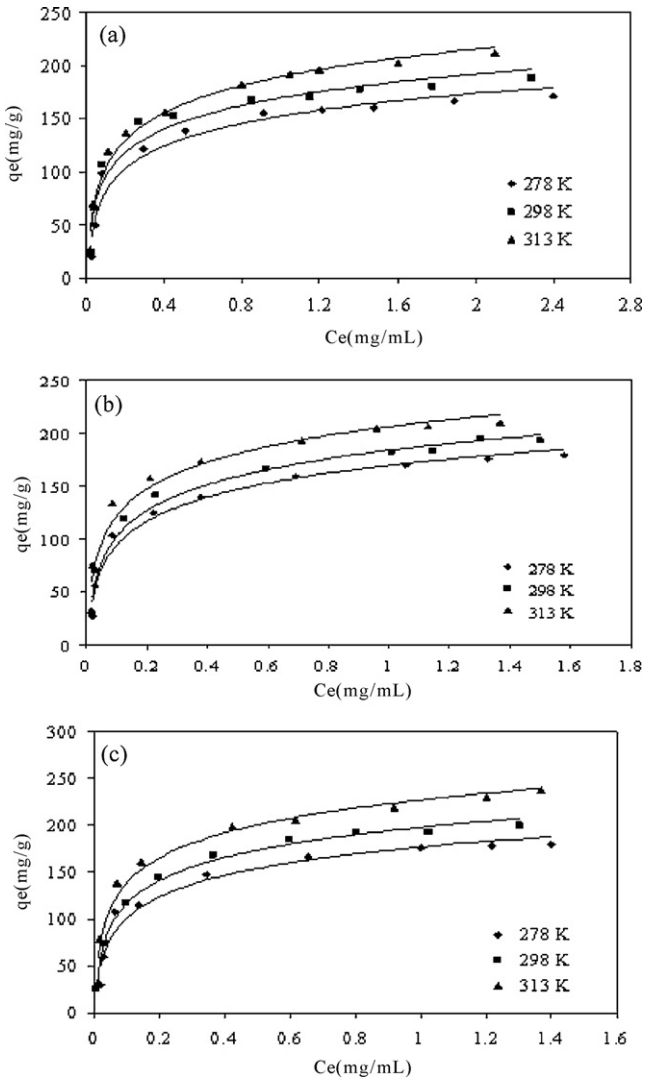

Fig. 9. Adsorption isotherms of MB by FN-PA (a), FN-PAG (b), FN-PAA (c) at temperatures of 278, 298, 313 K. Initial pH solution: 8.0 ± 0.1, pre-treatment pH: 11.0 ± 0.1, contact time: 200 min, nano-bioparticles dose: 5 g/L, agitation rate: 150 rpm.

form:

$$\frac{C_e}{q_e} = \frac{C_e}{Q_{max}} + \frac{1}{Q_{max}\, K_L} \quad (1)$$

where Q_{max} (mg/g) and K_L(L/mmol) are the maximum adsorption capacity and a measure of adsorption energy, respectively. Q_{max} and K_L are found from the slope and intercept of C_e/q_e versus C_e linear plot where K_L = (slope/intercept) and Q_{max} = 1/slope (see Table 1). q_e is the dye uptake (mg/g) that is obtained from the relation of $[(C_o - C_e)/(m/V)]$. q_e values were obtained as mean ± S.D. (n = 3) for each C_e, where C_o is the initial concentration of dye (mmol/L), m is the sorbent dry weight (g), V is the suspension volume (L) and C_e is the dye equilibrium concentration or un-adsorbed (mmol/L). As seen in Table 2, Q_{max} and K_L were determined as follows: FN-PAA > FN-PAG > FN-PA for each temperature which can show firstly, the importance of the cross-linking role of pectin to reach a better performance, secondly, the effect of the excess carboxyl presence in the probable and possible situations (b′) and (d′) in FN-PAA (see Fig. 1).

As seen in Fig. 9a–c, the MB uptake by each nano-biosorbent increases with increasing temperature for every initial MB concentrations. This can be due to the dissociation of proton from functional groups on the surface of pectin such as –COOH, leading to a higher availability of active sites at a higher temperature [35].

3.7. Kinetic study and modeling

To analyze the sorption kinetics, the first- and second-order kinetic models have been used. The first-order rate expression of Lagergren that shows the occupation rate of the adsorption sites is proportional to the number of unoccupied sites. The linearized form of the pseudo first-order model is written as

$$\log\ (q_e - q) = \log\ q_e - \left(\frac{k_{1,ads}}{2.303}\right) t \quad (2)$$

where q_e and q (mg/g) are the amount of adsorbed heavy metals on the adsorbent at equilibrium and at time t (min) and $k_{1,ads}$ (1/min) is the rate constant of first-order sorption. Linear plots of log $(q_e - q)$ versus t indicate the applicability of this kinetic model. However, to adjust Eq. (2) to the experimental data, the value of q_e (equilibrium sorption capacity) must be pre estimated by extrapolating the experimental data to $t = \infty$.

The Lagergren first-order rate constant ($k_{1,ads}$) and the equilibrium amount of metal removed (q_e) determined from the model are presented in Table 1 along with the corresponding correlation coefficient. However, the most important feature of this model is that it fails to estimate q_e. The linearized form of the pseudo-second-order model is written as

$$\frac{t}{q} = \frac{1}{(k_{2,ads}\, q_e^2)} + \left(\frac{1}{q_e}\right) t \quad (3)$$

where $k_{2,ads}$ (g/mg min) is the rate constant of second-order sorption. The plot t/q versus t should give a straight line if second-order kinetics are applicable and q_e and $k_{2,ads}$ can be determined from the slope and intercept of the plot, respectively.

Both parameters and the correspondent coefficients of correlation are also presented in Table 1. The correlation coefficients for the second-order kinetic model are equal to 0.998 and 0.999 for MB uptake by FN-PA, FN-PAG and FN-PAA and the theoretical values of q_e also agree very well with the experimental ones. Both facts

Table 2
Adsorption isotherm and thermodynamic parameters to remove MB by FN-PA, FN-PAG and FN-PAA. Initial pH solution: 8.0 ± 0.1, pre-treatment pH: 11.0 ± 0.1, contact time: 200 min, nano-bioparticles dose: 5 g/L, agitation rate: 150 rpm.

Nano-bioparticle	T (K)	Q_{max} (mmol/g)	K_L (1/mM)	ΔG° (kJ/mol)	ΔH° (kJ/mol)	ΔS° (kJ/mol K)
FN-PA	278	0.455	4.56	−3.507		
	298	0.534	7.22	−4.890	15.040	0.06661
	313	0.606	9.35	−5.817		
FN-PAG	278	0.523	8.89	−5.050		
	298	0.641	10.80	−5.895	7.832	0.04618
	313	0.746	13.02	−6.678		
FN-PAA	278	0.589	17.46	−6.610		
	298	0.695	19.68	−7.382	5.667	0.04403
	313	0.812	23.05	−8.165		

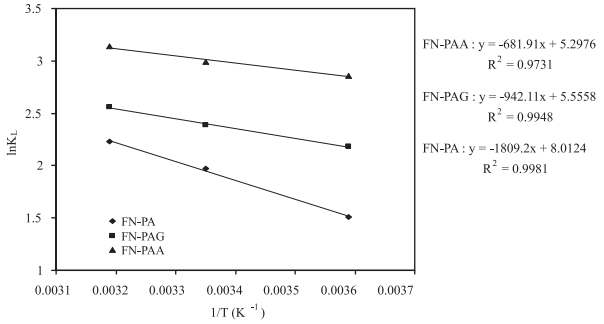

Fig. 10. Van't Hoff plots for the adsorption of MB onto nano-bioparticles.

suggest that the sorption of MB follows the second-order kinetic model, which relies on the assumption that adsorption may be the rate limiting step.

3.8. Thermodynamic study

According to the Van't Hoff equation:

$$\ln \quad K_L = \frac{-\Delta G^\circ}{RT} = \frac{-\Delta H^\circ}{RT} + \frac{\Delta S^\circ}{R} \tag{4}$$

Since K_L is the equilibrium constant, its dependence on temperature can be used to estimate both enthalpy change (ΔH°) and entropy change (ΔS°) associated to the sorption process.

The plot of $\ln K_L$ as a function of $1/T$ yields a straight line where ΔH° and ΔS° are found from the slope and intercept, respectively (see Fig. 10). R_g is the gas constant (8.314 J/mol K) and T is the absolute temperature. As seen in Table 2, the negative value of ΔG° confirms the spontaneous sorption and the positive ΔH° value shows the endothermic character of sorption processes. The positive value of ΔS° shows an increasing disorder at the interface between dye and sorbents.

It can be seen that the endothermic character of the MB uptake by the nano-bioparticles is as follows: FN-PAA < FN-PAG < FN-PA.

3.9. Activation energies comparison

The activation energy for MB adsorption by FN-PA, FN-PAG and FN-PAA were determined from the Arrhenius equation:

$$\ln \quad k = \frac{-\mathrm{Ea}}{RT} + \ln \quad A \tag{5}$$

where k is the rate constant according to the order of the fitted kinetic model for experiments (k is $k_{2,\mathrm{ads}}$ in this study, from Table 1), Ea is the activation energy (kJ/mol), T is the temperature (K), R is the gas constant (J/mol K) and A is a constant called the frequency or Arrhenius factor. The value of Ea can be determined from the slope of $\ln k_{2,\mathrm{ads}}$ versus $1/T$ plot (see Fig. 11). The magnitude of activation

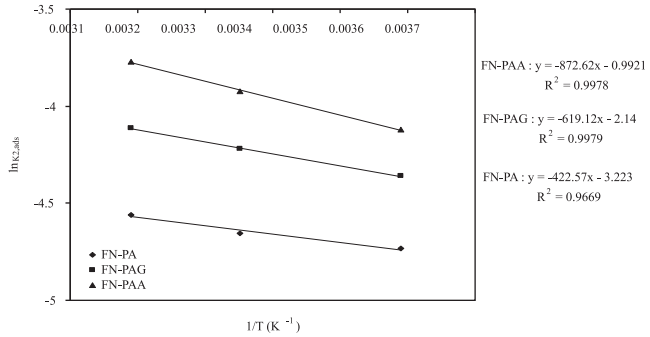

Fig. 11. Arrhenius plots for the adsorption of MB onto nano-bioparticles.

Table 3
Activation energy parameters for the adsorption of MB onto nano-bioparticles.

Nano-bioparticle	Ea (kJ/mol)	A
FN-PA	3.513	0.040
FN-PAG	5.147	0.117
FN-PAA	7.254	0.370

energy may give an idea about the type of the sorption. Chemical adsorption with high Ea viz. 60–800 kJ/mol, is specific and involves forces much stronger than those in physical adsorption with low Ea viz. 5–50 kJ/mol. Ea and A values to adsorb MB by FN-PA, FN-PAG and FN-PAA have been shown in Table 3. These results indicated that the adsorption of MB by nano-bioparticles were as the physical types. It also showed that the adsorption force of MB by these adsorbents is as follows: FN-PAA > FN-PAG > FN-PA. This arrangement is contrary to those endothermic characters (see Table 2).

4. Conclusions

On the basis of the experimental results of this investigation, the following conclusions can be drawn:

1. The removal of MB from aqueous solution by the modified Fe_3O_4 nano-particles with the extracted pectin from apple waste (FN-PA) increased due to using the cross-linked form of the pectin by glutaraldehyde (FN-PAG) and adipic acid (FN-PAA).
2. The results of XRD image indicate that the modification of Fe_3O_4 nanoparticles by pectin and cross-linked ones have not changed the crystal structure of nanoparticles. But the intensity of the peaks corresponding to surface functional groups is reduced by using pectin and cross-linking agents. This reduction for FN-PAA is more than FN-PAG.
3. The strong stretching band at 1120 cm^{-1} in spectra of FT-IR refers to C–O–C which is appeared after the reaction between –CHO groups (from glutaraldehyde) and –OH groups (from pectin). On the other hand, the stronger peak at 1730–1740 cm^{-1} in spectra of FN-PAA could be due to strengthening C=O band (esterified) after the reaction between –COOH groups (from adipic acid) and –OH groups (from pectin) and the excess –COOH groups.
4. The results of the FTIR study shows that the ratio of the free –COOH to the reacted –COOH with $-NH_2$ of the nano-particles surface in FN-PA is less than that for the nano-particles with the cross-linked pectin viz. FN-PAG and FN-PAA.
5. The uptake of MB on the nanoparticles increased rapidly within the first 30–50 min and reached an equilibrium after nearly 100 min.
6. The sorption capacity of MB on the nano-biosorbent decreased from 284.21 to 125.54 mg/g, 303.11 to 139.01 mg/g and 324.65 to 157.37 mg/g when the dosages of FN-PA, FN-PAG and FN-PAA were increased from 1.0 to 30 g/L, respectively.
7. The Langmuir constants ($Q_{\max}$ and K_L), kinetic constant (k_{ads}) and activation energy (Ea) to remove MB by nano-bioparticles at 278, 298 and 313 K were obtained as follows: FN-PAA > FN-PAG > FN-PA. But the enthalpy change (ΔH°) and entropy change (ΔS°) was as: FN-PAA < FN-PAG < FN-PA.
8. It was observed that increasing the pretreatment pH to 11.0 ± 0.1 increases the ability of nano-bioparticles to remove MB. On the other hand, the optimal adsorption pH was determined 8.0 ± 0.1.
9. The negative value of ΔG° confirms the spontaneous and the positive ΔH° value shows the endothermic character of sorption processes. The positive value of ΔS° shows an increasing disorder at the interface between dye and sorbents.

Acknowledgments

The authors are grateful to the Islamic Azad University, Mrs. M. Ebadi and Dr. Sina from Tehran University for their help and support.

References

[1] O. Ligrini, E. Oliveros, A. Braun, Photochemical processes for water treatment, Chem. Rev. 93 (1993) 671–698.
[2] U. Pagga, D. Brown, The degradation of dyestuffs. 2. Behavior of dyestuffs in aerobic biodegradation tests, Chemosphere 15 (1986) 479–491.
[3] J.M. Wang, C.P. Huang, H.E. Allen, D.K. Cha, D.W. Kim, Adsorption characteristics of dye onto sludge particulates, J. Colloid Interface Sci. 208 (1998) 518–528.
[4] S.Y. Oh, D.K. Cha, P.C. Chiu, B.J. Kim, Conceptual comparison of pink water treatment technologies: granular activated carbon, anaerobic fluidized bed, and zero-valent iron-Fenton process, Water Sci. 49 (2004) 129–136.
[5] S. Papic, N. Koprivanac, A.L. Bozic, A. Metes, Removal of some reactive dyes from synthetic wastewater by combined Al(III) coagulation/carbon adsorption process, Dyes Pigments 62 (2004) 291–298.
[6] P. Bayer, M. Finkel, Modeling of sequential groundwater treatment with zero valent iron and granular activated carbon, J. Contam. Hydrol. 78 (2005) 129–146.
[7] M. Alkan, M. Dogan, Y. Turhan, O. Demirbas, P. Turan, Adsorption kinetics and mechanism of maxilon blue 5G dye on sepiolite from aqueous solutions, Chem. Eng. J. 139 (2008) 213–223.
[8] A. Mittal, V.K. Gupta, A. Malviya, J. Mittal, Process development for the batch and bulk removal and recovery of a hazardous, water-soluble azo dye (Metanil Yellow) by adsorption over waste materials (Bottom Ash and De-Oiled Soya), J. Hazard. Mater. 151 (2008) 821–832.
[9] T. Zhou, Y.Z. Li, F.S. Wong, X.H. Lu, Enhanced degradation of 2,4-dichlorophenol by ultrasound in a new Fenton like system (Fe/EDTA) at ambient circumstance, Ultrason. Sonochem. 15 (2008) 782–790.
[10] J.R. Perey, P.C. Chiu, C.P. Huang, D.K. Cha, Zero-valent iron pretreatment for enhancing the biodegradability of azo dyes, Water Environ. Res. 74 (2002) 221–225.
[11] S.J. Allen, G. Mckay, J.F. Porter, Adsorption isotherm models for basic dye adsorption by peat in single and binary component systems, Colloid Interface Sci. 280 (2004) 322–333.
[12] G. Mckay, M. El-guendi, M.M. Nassar, Adsorption model for the removal of acid dyes from effluent by bagasse pith using a simplified isotherm, Adsorpt. Sci. Technol. 15 (1997) 251–270.
[13] G. Mckay, V.J.P. Poots, Kinetics and diffusion process in colour removal from effluent using wood as an adsorbent, J. Chem. Biotechnol. 30 (1980) 279–292.
[14] M. Rachakornkij, Removal of dyes using bagasse fly ash, J. Sci. Technol. 26 (2004) 14–20.
[15] Y. Fu, T. Viraraghavan, Column studies for biosorption of dye from aqueous solutions on immobilised *Aspergillus niger* fungal biomass, Water Sci. 29 (2003) 465–472.
[16] S. Schiewer, S.B. Patil, Pectin-rich fruit wastes as biosorbents for heavy metal removal: equilibrium and kinetics, Bioresour. Technol. 99 (2008) 1896–1903.
[17] T. Padmesh, K. Vijayaraghavan, G. Sekaran, M. Velan, Batch and column studies on biosorption of acid dyes on fresh water macro alga *Azolla filiculoides*, J. Hazard. Mater. B125 (2005) 121–129.
[18] R. Zhang, X. Wang, One step synthesis of multiwalled carbon nanotube/gold nanocomposites for enhancing electrochemical response, Chem. Mater. 19 (2007) 976–978.
[19] S. Ikeda, Y. Ikoma, H. Kobayashi, T. Harada, T. Torimoto, B. Ohtanic, M. Matsumura, Encapsulation of titanium(IV) oxide particles in hollow silica for size-selective photocatalytic reactions, Chem. Commun. 36 (2007) 3753–3755.
[20] T. Gao, Q. Li, T. Wang, Sonochemical synthesis, optical properties, and electrical properties of core/shell-type ZnO nanorod/CdS nanoparticle composites, Chem. Mater. 17 (2005) 887–892.
[21] F. Caruso, Nanoengineering of particle surfaces, Adv. Mater. 13 (2001) 11–22.
[22] C.M. Niemeyer, Nanoparticles, proteins, and nucleic acids: biotechnology meets materials science, Chem. Int. Educ. 40 (2001) 4128–4158.
[23] Y.T. Lin, C.H. Weng, F.Y. Chen, Effective removal of AB24 dye by nano/micro-size zero-valent iron, Sep. Purif. Technol. 64 (2008) 26–30.
[24] S.S. Banerjee, D.H. Chen, Fast removal of copper ions by gum Arabic modified magnetic nano-adsorbent, J. Hazard. Mater. 147 (2007) 792–799.
[25] S.H. Huang, D.H. Chen, Rapid removal of heavy metal cations and anions from aqueous solutions by an amino-functionalized magnetic nano-adsorbent, J. Hazard. Mater. 163 (2009) 174–179.
[26] F. Chivrac, E. Pollet, L. Aveïrous, Progress in nano-biocomposites based on polysaccharides and nanoclays, Mater. Sci. Eng. R 67 (2009) 1–17.
[27] A. Jauneau, M. Quentin, A. Driouich, Micro-heterogeneitly of pectins and calcium distribution in the epidermal and cortical *parenchyma* cell wall of flax hypocotyls, Protoplasma 189 (1997) 9–19.
[28] A. Kamnev, M. Colina, J. Rodriguez, Comparative spectroscopic characterization of different pectins and their source, Food Hydrocolloids 12 (1998) 263–271.
[29] A. Synytsya, J. Copikova, P. Matejka, V. Mackovic, Fourier transform Raman and infrared spectroscopy of pectins, Carbohydr. Polym. 54 (2003) 97–106.
[30] R. Rakhshaee, M. Giahi, A. Pourahmad, Studying effect of cell wall's carboxyl–carboxylate ratio change of *Lemna minor* to remove heavy metals from aqueous solution, J. Hazard. Mater. 163 (2009) 165–173.
[31] M.H. Liao, D.H. Chen, Preparation and characterization of novel magnetic nano-adsorbents, J. Mater. Chem. 12 (2002) 3654–3659.
[32] F. Ting Li, H. Yang, Y. Zhao, R. Xu, Novel modified pectin for heavy metal adsorption, Chin. Chem. Lett. 18 (2007) 325–328.
[33] M. Masmoudi, S. Besbes, M. Chaabouni, C. Robert, Optimization of pectin extraction from lemon by-product with acidified date juice using response surface methodology, Carbohydr. Polym. 74 (2008) 185–192.
[34] A. Round, N. Rigby, A. MacDougall, V. Morris, A new view of pectin structure revealed by acid hydrolysis and atomic force microscopy, Carbohydr. Res. 345 (2010) 487–497.
[35] K.S. Low, C.K. Lee, B.F. Tan, Quaternized wood as sorbent for reactive dyes, Appl. Biotechnol. 87 (2000) 233–245.